

# A NEW NON-ARCHIMEDEAN METRIC ON PERSISTENT HOMOLOGY

İSMAIL GÜZEL AND ATABEY KAYGUN

**ABSTRACT.** In this article, we define a new non-archimedean metric structure, called *cophenetic metric*, on persistent homology classes of all degrees. We then show that zeroth persistent homology together with the cophenetic metric and hierarchical clustering algorithms with a number of different metrics do deliver statistically verifiable commensurate topological information based on experimental results we obtained on different datasets. We also observe that the resulting clusters coming from cophenetic distance do shine in terms of different evaluation measures such as silhouette score and the Rand index. Moreover, since the cophenetic metric is defined for all homology degrees, one can now display the inter-relations of persistent homology classes in all degrees via rooted trees.

## 1. INTRODUCTION

In this article, we define a new non-archimedean metric (a.k.a. an ultra-metric) called *cophenetic metric* on persistent homology classes of all degrees using only homological information. Then we statistically verify that the topological information coming from the zeroth persistent homology with our cophenetic metric is consistent with the information provided by different hierarchical clustering algorithms using different metrics based on numerical experiments on different datasets. We also observe that the clusters we obtained via the cophenetic metric do yield competitive silhouette scores and the Rand indices in comparison with clusters obtained from other metrics.

Persistent homology is a new class of topological invariants that has found applications in statistical data analysis. Its computations rely on techniques from topology, algebraic topology, computational geometry, and computational linear algebra. In simplest terms, this class of invariants (recorded as a basis of a vector space) aim to keep a record of the topological features of the manifold that our data is sampled from such as the connected components, circle-like and higher dimensional sphere-like cavities. Moreover, the calculated topological invariants of the manifold from which our data is sampled come with a scale or a time parameter. This allows homology classes we computed to evolve as the parameter changes (creation, annihilation, merging, splitting etc.) and yields opportunities for heuristic fine-tuning depending on needs and computational constraints. Furthermore, while the scale parameter may interact with the ambient metric of the data space, since homological invariants are purely topological the persistent homology is impervious to any perturbations in the metric structure as well as the number of features of the data space. This may be useful in situations where the ambient metric needs to be adjusted depending on the constraints, or worse yet, where no such metric exists.

In the standard representation of persistent homology, one only keeps a record of the number of persistent homological classes in the form of *life-time intervals*, called *barcodes* [10]. However, persistent homology classes carry a very rich combinatorial structure, and one can do more than just counting them. In reference to the dendrograms of hierarchical clustering algorithms, Carlsson expresses the same idea as a question in [35, Ch.8] and [7]:

The dendrogram can be regarded as the “right” version of the invariant  $\pi_0$  in the statistical world of finite metric spaces. The question now becomes if there are similar invariants that can capture the notions of higher homotopy groups or homology groups.

Since hierarchical clustering schemes, and therefore, dendrograms and non-archimedean metrics are known to be equivalent by Carlsson [9], to answer this question it is clear that one needs to define a non-archimedean metric for homology or homotopy classes.

Our contributions. The main contribution of this paper is a new non-archimedean metric defined on persistent homology classes in all degrees using purely homological information coming from the changing scale parameter. For this metric, we analyze how persistent homology classes of a certain degree “merge” on top of recording the birth and death times of these classes as the scale parameter changes. We observe that since all data points naturally appear as zeroth degree persistent homology classes, one can compare our metric with standard distance measures with respect to their performances in machine learning algorithms that rely on distance measures on data points. We tested the soundness of our proposal by checking whether hierarchical clustering methods with different metrics do indeed yield statistically verifiable commensurate topological information. We observe that when we measure the clusters obtained from the cophenetic metric against the clusters coming from other metrics we obtained competitive results. Furthermore, the metric we define on the persistent homology can now be used to sketch rooted tree presentations of the persistent homology classes in all degrees that track how these classes *merge* as the scale parameter changes.

In forming the bridge between hierarchical clustering and persistent homology, we also found that the answer to the question raised by Carlsson [7] comes from algebraic topology: cobordisms. Dendrograms are 1-dimensional cobordism classes of disjoint union of points. For higher homology classes, one has to resort to  $n + 1$ -dimensional cobordisms of disjoint unions of  $n$ -spheres. For example, for persistent homology in degree 1 such cobordisms are given by oriented genus- $g$  Riemann surfaces with finitely many punctures, and the classification of such 2-manifolds is complete. Unfortunately, in dimensions 2- and higher such cobordisms are very difficult to classify. We are going to investigate the special case of persistent homology of degree-1 in an upcoming paper.

Prior art. Topological data analysis (TDA) is a new data analysis discipline whose fundamentals straddle both very abstract and concrete sub-disciplines of the mathematical research. Even though the theoretical roots TDA are firmly placed in algebraic topology, to solve its computational needs it heavily uses computational geometry and numerical linear algebra. Since TDA relies on the topology rather than a particular metric structure of the ambient space from which data is sampled, in theory, it is more suitable for extracting information from data for which a canonical metric is not clear from the context, or worse yet, does not exist.

Clustering algorithms, on the other hand, have been around for a long time and they form an important and well-understood class of machine learning algorithms [24, 29, 30, 45]. They are known to be equivalent to non-archimedean metrics [9]. For a given data set, these algorithms aim to deliver an optimal partition where subsets are supposed to show a high degree of heterogeneity between, and a high degree of homogeneity within each subset. However, one has to make unavoidable ad-hoc choices to determine an optimal hierarchical clustering algorithm for any data set at hand due to the impossibility result of Kleinberg [27].

Similar to clustering algorithms, the TDA methods we investigate in this paper also rely on a changing scale parameter. But instead of relying on the metric structure alone, these methods

propose using *persistent homology* to compute topological invariants of a data set. Persistent homology was first introduced to investigate topological simplifications of alpha shapes in [15], but later extended to arbitrary dimensional spaces in [51]. The topological invariants that persistent homology identifies are *the Betti numbers* defined for every natural number  $n$ . For instance, the Betti numbers for  $n = 0, 1$  and  $2$  indicate respectively the number of connected components, 2- and 3- dimensional holes within the data set. The information that persistent homology yields on the change in topological features as the filtration scale parameter increases can be presented in various different ways by barcodes [10] and [20], by persistence diagrams [12], by landscapes [5], by images [1], by terraces [36], by entropy [34] and by curves [11]. Barcodes are the most commonly used representations of persistent homology classes in which one keeps a record of finite collections of scale parameter intervals over which individual persistent homology classes *persist*.

Hierarchical clustering algorithms that we consider in this paper extract their results based solely on the metric structure of the ambient space where the data set is embedded. One can also statistically test the stability and convergence of these methods [8, 9]. In addition, they use a convenient tree representations, called *dendrograms*, to display the information on how these clusters merge as the underlying scale parameter changes [26]. One can compare dendrograms coming from different variants of clustering algorithms using a suitable metric [21, 24, 25], or even improve forecasts by comparing dendrogram-like features obtained from different hierarchical clustering methods on the same data set [23].

In [16], the authors develop diagrams called *mergegrams* derived out of the dendrograms of the hierarchical clustering algorithms as a replacement for the zeroth bar code. However, unlike the mergegrams that depend on the metric structure of the ambient space and work with the zeroth bar codes only, our non-archimedean metric relies on purely homological information and are defined for all persistent homology degrees. More importantly, they can be used for purposes other than sketching rooted tree presentations.

Plan of the article. This paper is organized as follows. We give the necessary background material we need on persistent homology and hierarchical clustering in Sections 2 and 3. We outline our methodology in Section 4. The results of our numerical experiments<sup>1</sup> are given in Section 5, and in Section 6 we present our detailed analysis of our experimental work in the light of theoretical discussions we presented in the earlier sections. We also propose several avenues of future work in the same Section.

## 2. PERSISTENT HOMOLOGY

**2.1. Point clouds and simplicial complexes.** In hierarchical clustering, a collection of points given in an ambient metric space carries no information other than the distances between them. Derived information such as cophenetic matrices also rely on this metric structure. However, there are other tools to derive more information about the topology of the data set at hand. One of these useful tools one can use is a *simplicial complex*.

An abstract simplicial complex  $K$  in a space  $X$  is a collection of subsets of  $X$  such that for any two  $x, y \in K$  one also has  $x \cap y \in K$ . There are two variants of simplicial complexes that are of interest for us: Vietoris-Rips complexes and Čech complexes.

---

<sup>1</sup>The source code and the data of the numerical experiments we conducted in the paper can be found on the authors' GitHub page at <https://github.com/ismailguzel/TDA-HC>.

2.1.1. *Vietoris-Rips complexes.* Given a point cloud  $D$ , the Vietoris-Rips is defined to be the simplicial complex whose simplices are all points in  $D$  that are at most  $\varepsilon$  apart.

$$R_\varepsilon(D) = \{\sigma \subset D \mid d(x, y) \leq \varepsilon, \text{ for all } x, y \in \sigma\}$$

2.1.2. *Čech complexes.* Given a point cloud  $D$ , the Čech complex associated with  $D$  is defined to be the simplicial complex given by

$$C_\varepsilon(D) = \left\{ \sigma \subseteq D \mid \bigcap_{x \in \sigma} B_\varepsilon(x) \neq \emptyset \right\}.$$

In other words, a collection of points  $\sigma = (x_0, \dots, x_\ell)$  forms an  $\ell$ -simplex if the set of balls of radius  $\varepsilon$  centered at these points has non-empty intersection.

2.2. **Choosing an appropriate scale parameter.** In order to turn a point cloud  $D$  into a simplicial complex, we are going to use  $R_\varepsilon(D)$  the Vietoris-Rips complex associated with  $D$  with a chosen proximity parameter  $\varepsilon > 0$ . We then try to capture the topological features of the data by changing the parameter  $\varepsilon$ . As we see in Figure 1, we may not capture all of the topological features of data for a given proximity  $\varepsilon$ . Finding the optimal value for  $\varepsilon$  for a given data set  $D$  is a challenging problem.

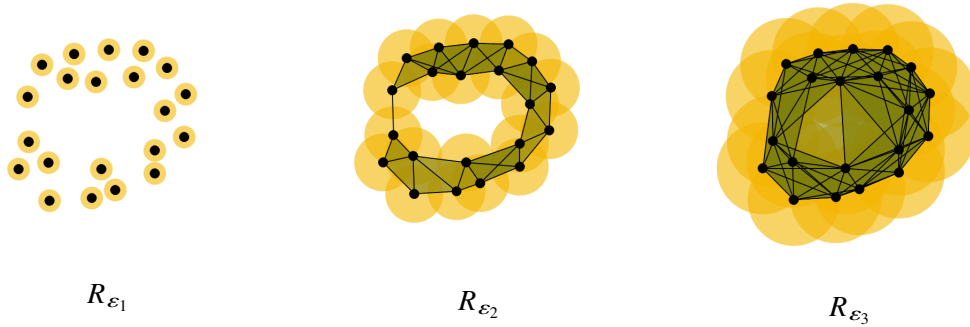


FIGURE 1. Vietoris-Rips complexes with increasing values of the parameters.

In [15] and [51], the authors proposed that the persistence homology might help to determine an optimal value for  $\varepsilon$ . In persistent homology, one records the longevity of each topological feature (in this case homology classes of  $R_\varepsilon(D)$ ) of a given data set as the proximity parameter  $\varepsilon$  changes. One does this by observing the *persistence* of these topological features depending on  $\varepsilon$ .

2.3. **Persistent Homology.** Let  $\{K_\varepsilon \mid \varepsilon \in \mathbb{R}_+\}$  be a filtration on a simplicial complex. In other words, each  $K_\varepsilon$  is a simplicial complex with  $K_\varepsilon \subseteq K_\eta$  for every  $\varepsilon < \eta$ , and we have  $K = \bigcup_{\varepsilon > 0} K_\varepsilon$ . The  $k$ -th persistent homology of  $K$  is given by

$$\text{PH}_k(K) := \{H_k(K_\varepsilon)\}_{\varepsilon \in \mathbb{R}_+}$$

together with the collection of linear maps  $\psi_{\varepsilon, \eta}^k : H_k(K_\varepsilon) \rightarrow H_k(K_\eta)$  induced by the inclusion maps of  $K_\varepsilon \hookrightarrow K_\eta$  for all  $k \in \mathbb{N}$  and  $\varepsilon < \eta$  in  $\mathbb{R}_+$ .

**2.4. Bar codes.** Persistent homology produces a collection of intervals depending on the parameter  $\varepsilon$  where we store the *life-time* of topological features of the point cloud via persistent homology. Here by *life-time* we mean the interval on which a homology cycle is non-trivial as  $\varepsilon$  ranges from 0 to  $\infty$ . We record both the *birth*, i.e when a topological feature appears, and the *death*, i.e when a topological feature disappears, as  $\varepsilon$  increases. To illustrate the life-time, we use *barcodes* as introduced by [10] and [20].

In a barcode, we place the basis vectors for the homology on the vertical axis whereas the horizontal axis represents the life span of each basis element in terms of the scale parameter  $\varepsilon$ . When we draw the vertical line at a particular  $\varepsilon_i$ , the number of intersecting line segments in a barcode is the dimension of the corresponding homology group, i.e. the Betti number, for that parameter  $\varepsilon_i$ . See Figure 2.

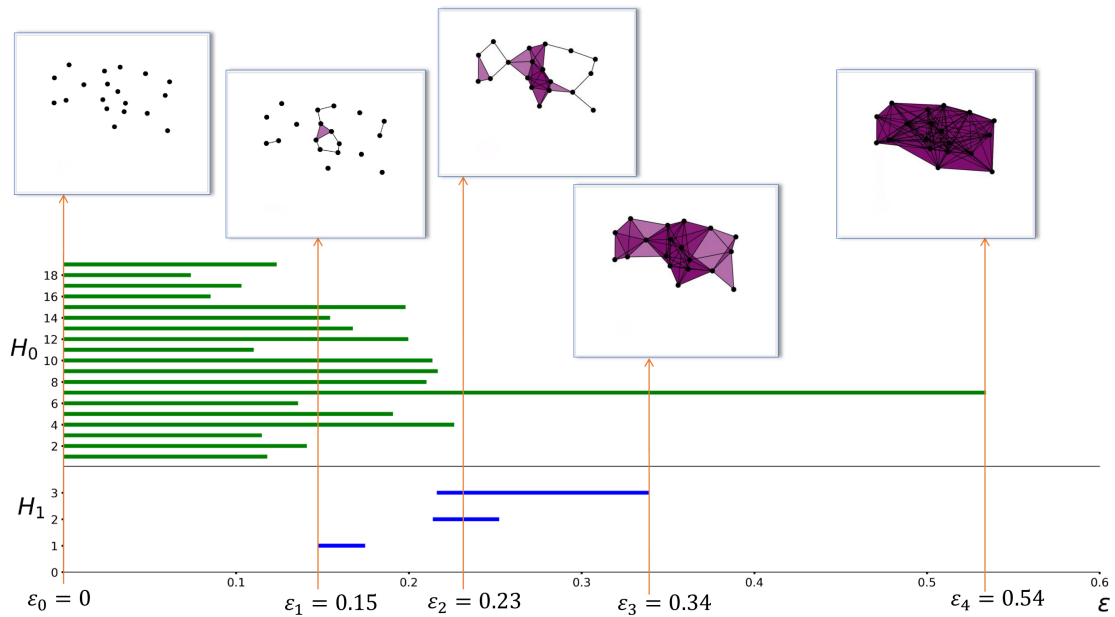


FIGURE 2. An example barcode.

In Figure 2, one can see barcodes for zeroth and first persistent homology together with the Vietoris-Rips complex corresponding to a particular  $\varepsilon$ . For example, the blue horizontal line whose left endpoint on 0.22 and right endpoint is on 0.25 represents a nonzero element in  $H_1(R_{0.22})$  that persisted until  $H_1(R_{0.25})$  at which point it either disappeared or merged with another class.

We will postulate that the longest living topological features in the barcode are the genuine topological features of the point cloud, whereas the shorter ones can be seen as artificial artifacts of the method we use. Notice also that there will always be one connected component as  $\varepsilon$  grows large, i.e. the zeroth Betti number  $\beta_0$  is always going to be 1 eventually.

### 3. HIERARCHICAL CLUSTERING

Assume we have a connected metric space  $(X, d)$ , and let  $\pi_0(X)$  be the set of connected components of  $X$ . Assume we have a finite random sample of points  $D \subseteq X$  taken from  $X$  whose distribution we do not know. Our aim is to deduce any information about the set of connected components of  $X$  using  $D$ . We are going to do this by finding a *finite clustering* of  $D$

which is a set function  $c : D \rightarrow \mathbb{N}$  such that each cluster  $c^{-1}(i)$  lies within a distinct connected component for each  $i \in \mathbb{N}$ .

**3.1. Hierarchical clustering.** In its simplest form, in hierarchical clustering we have a function  $c_\varepsilon : D \rightarrow \mathbb{N}$  for each scale parameter  $\varepsilon > 0$ . This function satisfies  $c_\varepsilon(x) = c_\varepsilon(y)$  for any two points  $x, y \in D$  when there is a sequence of points  $x_0, \dots, x_m \in D$  such that  $d(x_i, x_{i+1}) < \varepsilon$  for every  $i = 0, \dots, m-1$  where  $x_0 = x$  and  $x_m = y$ . Notice that the clustering algorithm is monotone in the sense that if  $c_\varepsilon(x) = c_\varepsilon(y)$  then  $c_\eta(x) = c_\eta(y)$  for every  $\eta > \varepsilon$ . Moreover, since  $D \subseteq X$  is finite and  $X$  is connected, there is a large enough scale parameter  $\varepsilon > 0$  such that the image of  $c_\varepsilon$  is a single cluster.

```

procedure CLUSTER( $Data, \varepsilon$ )
   $C \leftarrow \emptyset$ 
  for  $x$  in  $Data$  do
    Add  $\{x\}$  as a cluster to  $C$ 
  end for
  repeat
    Find a distinct pair  $(C_i, C_j)$  in  $C$  such that  $d(C_i, C_j) < \varepsilon$ 
    Remove the clusters  $C_i$  and  $C_j$  from  $C$ 
    Add the new cluster  $C_i \cup C_j$  to  $C$ 
  until  $d(C_i, C_j) \geq \varepsilon$  for all clusters
  return  $C$ 
end procedure

```

FIGURE 3. Clustering function pseudocode.

**3.2. Linkage in hierarchical clustering.** As we increase the scale parameter  $\varepsilon > 0$  we start forming *clusters* of points. Since we replace points with clusters, we are going to need to calculate distances between clusters. See Algorithm 3.

For a fixed  $\varepsilon > 0$ , let us use  $C_i = c_\varepsilon^{-1}(i)$  to denote a cluster, and set  $n_i = |C_i|$ . Let us use  $d_{ij}$  for the distance between the cluster  $C_i$  and  $C_j$ . Lance and Williams [29] introduced to the following general formula for calculating distances between clusters

$$d_{(ij)k} = \alpha_{ijk}d_{ik} + \alpha_{jik}d_{jk} + \beta_{ijk}d_{ij} + \gamma|d_{ik} - d_{jk}|$$

for parameters  $\alpha_{ijk}$ ,  $\beta_{ijk}$  and  $\gamma$  to be determined. Here,  $d_{(ij)k}$  denotes the distance between the clusters  $C_k$  and  $C_{ij} = C_i \cup C_j$  which is merged in a single cluster. We list the parameters for commonly used methods of calculating distances between clusters in Table 1. See [29] for details.

**3.3. Evaluation of clusters.** Performance evaluations in supervised learning tasks are easier and more understandable than unsupervised learning tasks such as clustering. However, there are also some useful metrics one can use to evaluate clustering tasks. In this subsection, we are going to review the metrics we are going to use to evaluate our classification and clustering algorithms. Particular metrics we are going to review are the mutual information [48], Rand index [22], and homogeneity, completeness [41], and the silhouette scores [42].

For this subsection, assume  $X$  is the random variable that designates the true labels  $\mathcal{X} = \{x_1, \dots, x_n\}$  while  $Y$  is the random variable that designates the predicted labels  $\mathcal{Y} = \{y_1, \dots, y_m\}$  of a classification task. Let  $\tau(d)$  be the true label and  $\pi(d)$  be the predicted label of a data

TABLE 1. Commonly used methods to determine  $d_{(ij)k}$ .

Linkage	$\alpha_{ijk}$	$\beta_{ijk}$	$\gamma$
Single	$\frac{1}{2}$	0	$-\frac{1}{2}$
Complete	$\frac{1}{2}$	0	$\frac{1}{2}$
Average	$\frac{n_i}{n_i + n_j}$	0	0
Ward	$\frac{n_i + n_k}{n_i + n_j + n_k}$	$\frac{-n_k}{n_i + n_j + n_k}$	0

point  $d$ . We use  $H(Z)$  to denote the Shannon entropy of a discrete random variable  $Z$  which is defined as

$$H(Z) = - \sum_{z \in Z} p(z) \log p(z).$$

Mutual information: The mutual information of the pair of the random variables  $X$  and  $Y$  is given as

$$MI(X, Y) = H(X) + H(Y) - H(X, Y)$$

Let  $C_x = \tau^{-1}(x)$  be the set of samples with true label  $x \in \mathcal{X}$  of size  $n_x$ , and let  $C_y = \pi^{-1}(y)$  be the set of samples with predicted label  $y \in \mathcal{Y}$  of size  $n_y$ . The joint distribution  $p(X = x, Y = y)$  which is an observation drawn at random falls into clusters  $C_x$  and  $C_y$  turn out to be  $\frac{|C_x \cap C_y|}{n}$  with the marginal probability  $p(X = x) = \frac{n_x}{n}$  and  $p(Y = y) = \frac{n_y}{n}$ . So, the mutual information of the pair  $(X, Y)$  can be written in terms of these cardinalities as

$$MI(X, Y) = \sum_{x \in \mathcal{X}} \sum_{y \in \mathcal{Y}} \frac{|C_x \cap C_y|}{n} \log \left( \frac{n|C_x \cap C_y|}{n_x n_y} \right).$$

Homogeneity and completeness: If all clusters contain only data points that are members of a single class, then we say that our clusters are homogeneous. On the other hand, if the data points that are members of a given class are elements of the same cluster then we say that our clusters are complete. Formally, the homogeneity and completeness scores are respectively defined by:

$$hom(X, Y) = 1 - \frac{H(X | Y)}{H(X)} \quad \text{and} \quad comp(X, Y) = 1 - \frac{H(Y | X)}{H(Y)}$$

Notice that both homogeneity and completeness scores are not affected by permutations of labels.

Rand index: The Rand index counts sample of unordered distinct pairs of data points  $\{u, v\}$  for which  $\tau$  and  $\pi$  agree, and also disagree. Formally, the Rand index is defined as

$$RI = \frac{a + b}{\binom{n}{2}},$$

where

$$a = |\{\{u, v\} : \tau(u) = \tau(v) \text{ and } \pi(u) = \pi(v)\}|$$

and

$$b = |\{\{u, v\} : \tau(u) \neq \tau(v) \text{ and } \pi(u) \neq \pi(v)\}|$$

and  $\binom{n}{2}$  is the total number of different possible unordered pairs in the dataset.

**Silhouette score:** We are going to use the silhouette score as defined in [42] to evaluate a clustering model on a dataset.

Assume we have a set of clusters  $C_1, \dots, C_k$ , and a dissimilarity measure  $d(x, y)$  for every pair of points in our dataset. Let  $U(x) = \pi^{-1}\pi(x)$  be the cluster that  $x$  belongs to and let

$$d(x, C_j) = \frac{1}{|C_j|} \sum_{y \in C_j} d(x, y)$$

The silhouette score  $s(x)$  of a point  $x$  in our dataset is given by the ratio

$$s(x) = \frac{a(x) - b(x)}{\max(a(x), b(x))}$$

where

$$a(x) = d(x, U(x)) \text{ and } b(x) = \min_{C \neq U(x)} d(x, C).$$

Silhouette scores take values in the interval  $[-1, 1]$  and values closer to 1 indicate that clusters are *well-formed*: they show low average intra-class similarity while maintaining a high average inter-class dissimilarity.

#### 4. A BRIDGE BETWEEN PERSISTENT HOMOLOGY AND HIERARCHICAL CLUSTERING

**4.1. Cophenetic matrix.** An important notion we need in studying and comparing clustering methods is *the cophenetic matrix* as defined in [24, 45, 46].

Assume we have a clustering function  $c_\varepsilon: D \rightarrow \mathbb{N}$ , and let  $C = \{C_i = c_\varepsilon^{-1}(i) \mid i \in \mathbb{N}\}$ . Let  $\varepsilon_{ij}$  be the proximity level at which the clusters  $C_i$  and  $C_j$  merge to form  $C_{ij}$  for the first time. We record these numbers in the cophenetic matrix  $C_\varepsilon(D) = (\varepsilon_{ij})$  for any pair of clusters  $C_i$  and  $C_j$ . The cophenetic distance is a metric under the assumption of monotonicity [44].

**4.2. Homological cophenetic distance.** Given a point cloud  $D$ , we consider the Vietoris-Rips complex  $R_\varepsilon(D)$ . By gradually increasing  $\varepsilon$ , we get a filtered simplicial complex, and thus, we can calculate the persistent homology associated with this filtration.

Recall that when we have a filtered simplicial complex  $\{R_\varepsilon\}_{\varepsilon > 0}$ , we have homology groups  $\{H_k(R_\varepsilon)\}_\varepsilon$  and connecting linear maps  $\psi_{\varepsilon, \eta}^k: H_k(R_\varepsilon) \rightarrow H_k(R_\eta)$  for every pair  $\varepsilon < \eta$  and for every  $k \in \mathbb{N}$ . We would like to emphasize that even though  $R_\varepsilon \subseteq R_\eta$  the induced maps in homology  $\psi_{\varepsilon, \eta}^k$  need not be injections.

Now, for each linearly independent pair of homology classes  $\alpha$  and  $\beta$  in  $H_k(R_\varepsilon)$  one can test if  $\psi_{\varepsilon, \eta}^k(\alpha)$  and  $\psi_{\varepsilon, \eta}^k(\beta)$  are still linearly independent in  $H_k(R_\eta)$ . If the pair  $\psi_{\varepsilon, \eta}^n(\alpha)$  and  $\psi_{\varepsilon, \eta}^n(\beta)$  is non-zero and fails to be linearly independent then we will say that two classes  $\alpha$  and  $\beta$  merged at time  $\eta$ .

**Definition 1.** *k*-th homological cophenetic distance is defined as

$$D_k(\alpha, \beta) = \inf \{ \eta - \varepsilon \geq 0 \mid \psi_{\varepsilon, \eta}^k(\alpha) \text{ and } \psi_{\varepsilon, \eta}^k(\beta) \text{ are non-zero and linearly dependent} \}.$$

**Proposition 1.** *The cophenetic metric is non-archimedean:*

$$D_k(\alpha, \beta) \leq \max(D_k(\alpha, \gamma), D_k(\gamma, \beta))$$

for every  $\alpha, \beta, \gamma \in H_k(R_\varepsilon)$ .



**4.3. Non-archimedean metrics and hierarchical clustering.** It has been known that hierarchical clustering methods and non-archimedean metrics are intimately related [21, 24, 25]. But it was Carlsson and Memoli who proved that hierarchical clustering methods and non-archimedean metrics are naturally equivalent in [9]. The immediate corollary is that the homological cophenetic metric we defined in Definition 1 does correspond to a unique hierarchical clustering scheme on every homology group.

Recall that the connected components of a topological or a metric space  $X$  are encoded in the zeroth homology classes of  $X$ . This means, one can naturally compare various clustering schemes on a dataset embedded in  $X$  with the homological cophenetic distance for the zeroth homology by varying the underlying metric of  $X$  if the ambient space  $X$  allows it. The rest of the paper will follow this route.

Observe also that we have homological cophenetic distance for all homology groups, not just zeroth homology, which do not have obvious connections with the point clouds that form a dataset. Investigating the ramifications of the non-archimedean homological cophenetic distance for higher homology groups is going to be the subject matter of a subsequent paper.

**4.4. The zeroth homology and hierarchical clustering.** For the zeroth homology there is a simplification: all homology classes appear at  $\varepsilon = 0$  since every point is a connected component by itself, and they never disappear only merge as  $\varepsilon$  goes to  $\infty$  for the subsequent Vietoris-Rips complexes. Thus, it is enough to test whether the classes  $\psi_{0,\varepsilon}^0(\alpha)$  and  $\psi_{0,\varepsilon}^0(\beta)$  are linearly independent in  $H_0(R_\varepsilon)$  as  $\varepsilon$  varies.

We also note that each point  $x \in D$  is a homology class in  $H_0(R_0)$ , and these points mark the rows and columns of the cophenetic matrix  $C_0(D)$  coming from hierarchical clustering. As a consequence we can compare these matrices.

**4.5. Mantel Test.** As we stated above, we need to compare different dendrograms, or equivalently, different distance matrices on a given dataset. For this purpose we are going to use the Mantel test as defined in [32]. It is commonly used in biology and ecology to compare phylogenetic trees. Mantel test is a non-parametric statistical method that computes the significance of correlation between rows and columns of a matrix through permutations of these rows and columns in one of the input distance matrices.

We consider two distance or cophenetic matrices  $D_1 = (x_{ij})$  and  $D_2 = (y_{ij})$  of size  $n \times n$ . The normalized Mantel statistic  $r$  is defined as

$$r = \frac{2}{(n-2)(n+1)} \sum_{i=1}^n \sum_{j=i+1}^n \left( \frac{x_{ij} - \bar{x}}{s_x} \right) \left( \frac{y_{ij} - \bar{y}}{s_y} \right)$$

where

- (i)  $\bar{x}$  and  $\bar{y}$  are averages of all entries of each matrix, and
- (ii)  $s_x$  and  $s_y$  are the standard deviations for  $x$  and  $y$ .

The test statistic is the Pearson product-moment correlation coefficient  $r \in [-1, 1]$ . Having a value in the neighborhood of  $-1$  indicates strong negative correlation whereas  $+1$  indicates strong positive correlation, and  $0$  indicates no relation.

In order to estimate the sampling distribution of the standardized Mantel statistic under the null-hypothesis (no correlation between the distance matrices), random permutations of the rows (or equivalently columns) of the distance matrices are used to get a set of values of the statistic. Then whether the null-hypothesis is rejected depends on the value of the Mantel statistic: If

the calculated statistic is unlikely to have been obtained under the null-hypothesis then the null-hypothesis is rejected. See [30, Sect. 10.5] for details.

## 5. EXPERIMENTS

To determine if our research is sound, we performed numerical experiments<sup>2</sup> on synthetic and different real datasets. Statistically, we compare the dendrograms we obtained from the Euclidean distance and the dendrograms we obtained from the cophenetic distance for the zeroth persistent homology. Also, this statistically comparison methods is done for various distance metrics, too. On the other hand, we evaluate the clustering measurements from hierarchical clustering algorithm by changing the metrics on different datasets. In this section, we are going to summarize these experiments.

**5.1. A sample of cities in Turkey.** For our first experiment, we used a subset 24 of cities in Turkey whose coordinates are encoded as longitudes and latitudes in radians. See Figure 4.



FIGURE 4. A sample of cities in Turkey

**5.1.1. Bar codes and dendrograms.** The left hand side of Figure 5 is the dendrogram we obtained from cophenetic homological distance matrix for the zeroth homology. The right hand side of Figure 5 is the ordinary barcode obtained from the zeroth persistent homology which displays the birth and death times of each homology class, whereas the left hand side is the dendrogram that indicates which classes merge.

**5.1.2. Comparison of Dendrograms.** Next, we apply the hierarchical clustering (with single linkage), using the Euclidean distance matrix  $E(D)$ , and the homological cophenetic distance matrix  $C_0(D)$  for the zeroth persistent homology. The resulting dendrograms are given in Figure 6. We also align the labels from both dendrograms without changing the underlying cluster structure. In a tanglegram representation, one compares the tree structures using a metric derived from matches between labels placed on branches [6, 17, 43].

<sup>2</sup>The computational tools we use in this section are as follows: To compare dendrograms, we use tools come from the **dendextend** [19] and **vegan** [37] packages of the R programming language [40]. For the map of Turkey, we used Generic Mapping Tools [50]. To compute cophenetic distance matrix we used SageMath [13]. In order to compute and visualize clusters, we used python programming language [49] and its **scikit-learn** library [39].

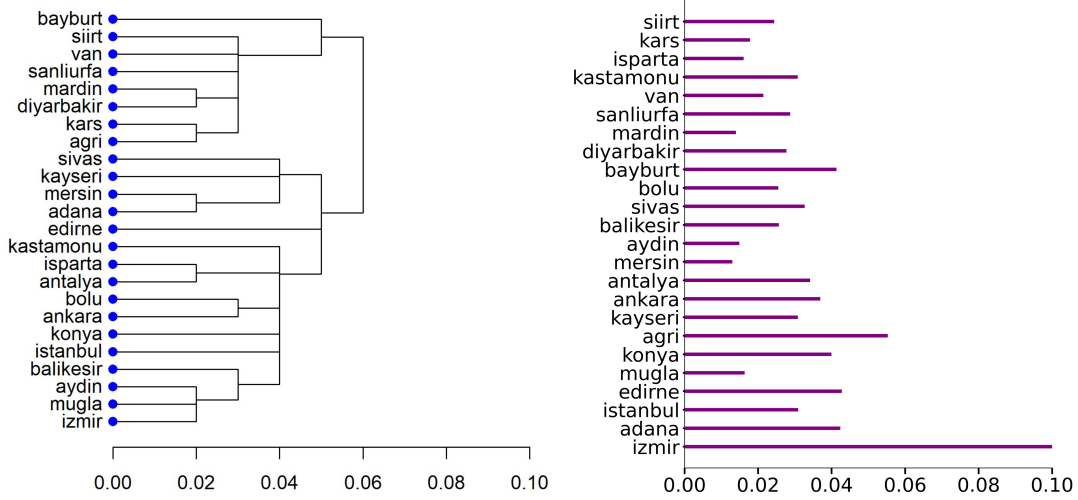


FIGURE 5. Hierarchical enriched barcodes and classical barcodes in TDA

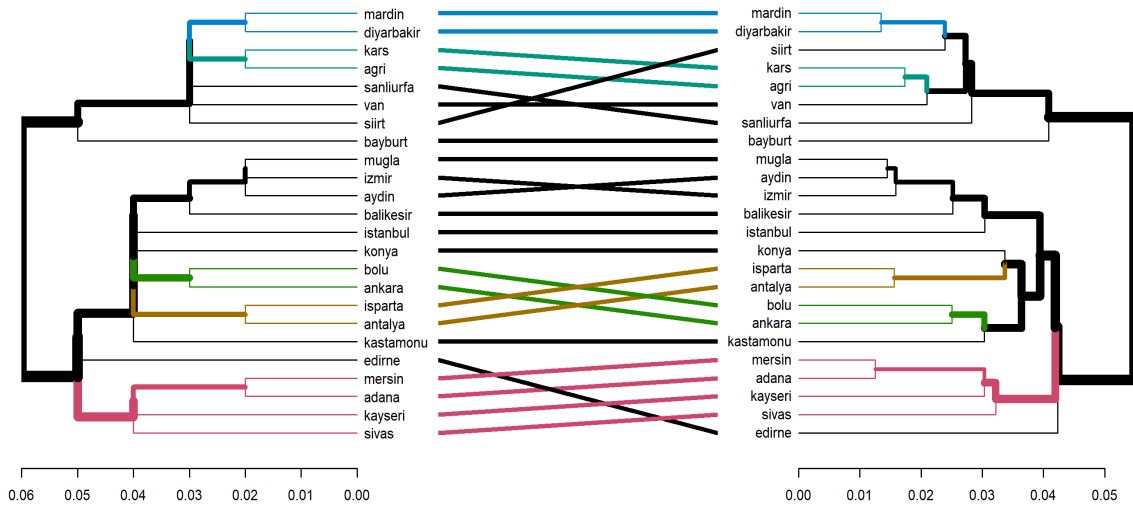


FIGURE 6. Tanglegram of the dendrograms of the cophenetic (left) and Euclidean distances (right).

For the next phase, we need to compare dendrograms. We are going to use the Mantel test (See Section 4.5) for this task. The resulting statistic is a measure of how well the labels of the two dendrograms are aligned. For the sample of cities we used, the Mantel statistic value we obtained for the matrices  $E(D)$  and  $C_0(D)$  was 0.98 with p-value of 0.001.

5.1.3. *A full comparison of metrics.* In Section 5.1.2, we explicitly compared cophenetic homological metric with the Euclidean metric. In this section, we extend the comparison to a variety of metrics. As we discussed in Section 4.5, we are going to use the Mantel test for this comparison.

For our comparisons we used the  $L^2$ -metric (also known as the *Euclidean metric*), the  $L^1$ -metric (also known as *taxicab distance*, *city-block distance*, or the *Manhattan distance*),  $L^p$ -metric (also known as the *Minkowski distance*) with  $p = 1/2$ , the cosine similarity converted to a

dissimilarity function, and Bray-Curtis dissimilarity [4], and [30, Eq. 7.58]. Our resulting Mantel test table is given in Table 2.

TABLE 2. Mantel statistics of metrics on the cities of Turkey dataset.

PAIRWISE MANTEL STATISTICS						
Metrics	Bray-Curtis	Cosine	Manhattan	Euclidean	Minkowski	Homological
<b>Bray-Curtis</b>	1.00	0.64	0.96	0.90	0.90	0.90
<b>Cosine</b>		1.00	0.61	0.52	0.69	0.59
<b>Manhattan</b>			1.00	0.96	0.87	0.97
<b>Euclidean</b>				1.00	0.75	0.98
<b>Minkowski</b>					1.00	0.78
<b>Homological</b>						1.00

The results indicate that our homological cophenetic distance, produce results most similar to the Euclidean metric and the Manhattan metric, and is most dissimilar to the cosine similarity. Homology is a topological invariant, and therefore, is impervious in any perturbations of the underlying metric structure. However, the filtration structure on the Rips complexes we used rely heavily on the underlying metric. Thus one can surmise that, the main contributing factor for this similarity might be the fact that we used Euclidean metric when we formed Rips complexes.

## 5.2. Cophenetic distance on different datasets.

TABLE 3. Datasets used and their properties.

Dataset	#Instances	#Attributes	Supervised	#Classes
Turkish Cities	82	2	No	-
Iris	150	4	Yes	3
Cancer Coimbra	116	10	Yes	2
Synthetic (total separation)	100	100	Yes	4
Synthetic (with mixture)	100	2	Yes	4

In the previous section, we compared the dendrograms coming from different metrics on the coordinates of a small sample cities in Turkey. In this section, we are going to evaluate the clusters coming from hierarchical clustering algorithms by varying the metrics on 5 different datasets: all cities in Turkey, the *Iris Dataset* [18], the *Cancer Coimbra Dataset* [38] and two synthetic datasets that we generated. One of these synthetic datasets has 4 linearly separable clusters, and the other contains 4 clusters with mixing along their boundaries. For the synthetic datasets we used `make_blobs` function from the scikit-learn library [39] of the python language [49].

**5.2.1. Silhouette scores.** In order to compare the resulting clusters on each dataset, we are going to use silhouette scores as discussed in Section 3.3. The results of average silhouette scores for different number of clusters given in Figure 7.

The graphs in Figure 7 indicate that one must consider the silhouette score and the *marginal* silhouette scores simultaneously in order to determine the right number of clusters. For the synthetic datasets, the cophenetic metric produced the best silhouette scores. We also see that the silhouette score did indeed determine the right number of clusters for both of the synthetic datasets regardless of the choice of the metric. For the Iris datasets, all metrics appear to produce comparable silhouette scores. In this case, the cophenetic metric suggests that the right number is 4 while other metrics agree on 2 clusters. We touch on this issue in the Conclusion. On the other hand, the consensus on the right number of clusters for the Cancer dataset is 2 for all

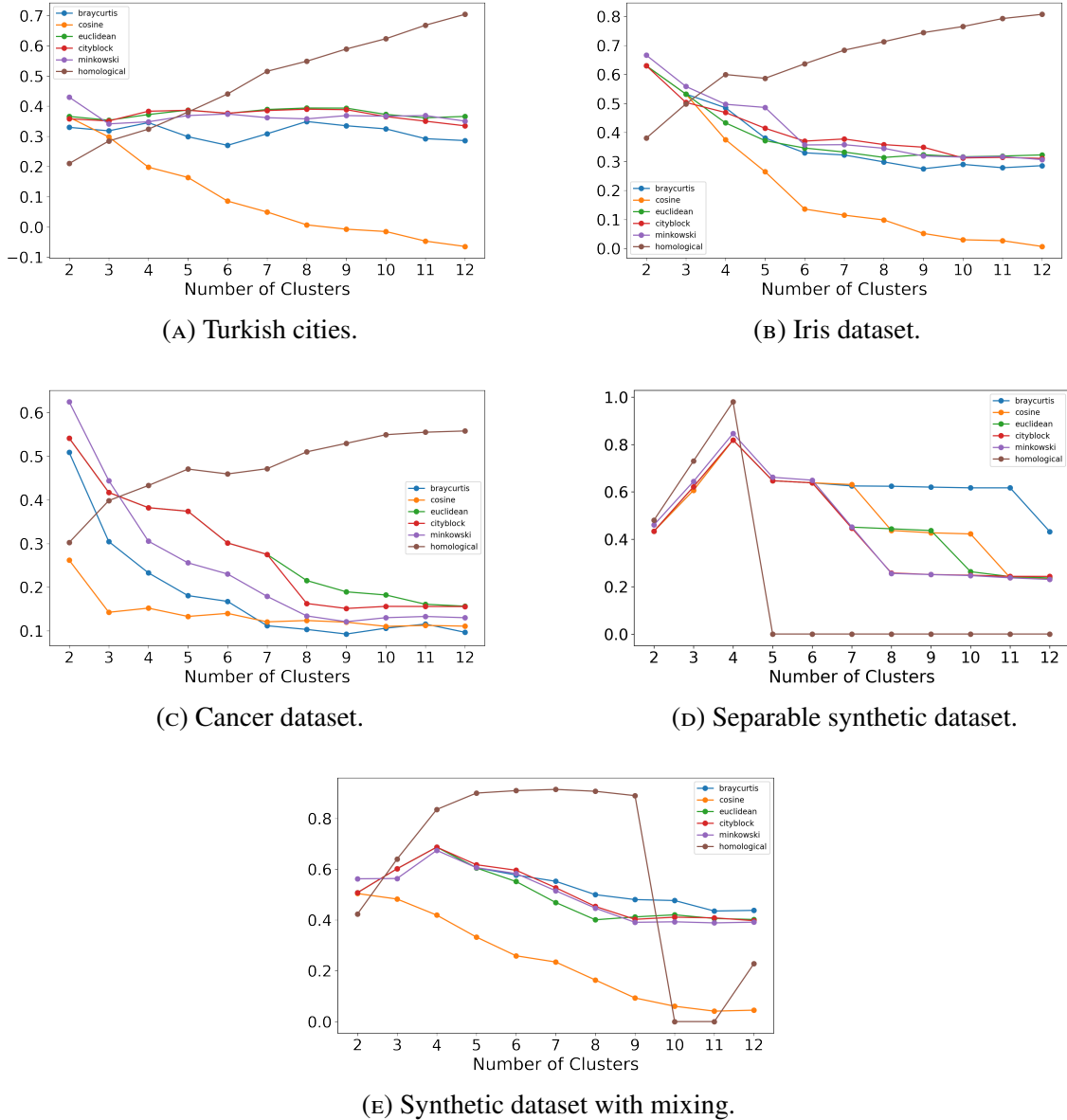


FIGURE 7. Silhouette scores for each dataset.

metrics while cophenetic metric suggests 5. Finally, there appears to be no meaningful clusters for the Turkish cities dataset.

5.2.2. *Linkages.* There is one more parameter that effects the forming of clusters: the linkages we use to calculate the distances between newly merged clusters as discussed in Section 3.2. For this set of experiments, we used hierarchical clustering on each dataset using different linkage methods.

Since hierarchical clustering is an unsupervised method, to use measures such as the F1-score and accuracy, we need to find a suitable permutation of the confusion matrix for each dataset. To deal with this problem, we use the Hungarian assignment method as defined in [28]. We then evaluate each model using F1-score (F1), accuracy (Acc.), homogeneity (Hom.), completeness (Comp.) [41], mutual information (M.Info) [48] and Rand index (Rand) [22]. We display our results in Table 4. In each table, we report the best performing linkage method (single (S),

TABLE 4. A comparison of metrics on datasets.

(A) Iris dataset.

<b>Metric</b>	<b>F1</b>	<b>Acc.</b>	<b>Hom.</b>	<b>Comp.</b>	<b>M.Info</b>	<b>Rand</b>
bray-curtis	0.82 W	0.88 W	0.69 W	0.95 S	0.75 S	0.82 W
cosine	0.68 W	0.79 W	0.58 W	0.95 S	0.64 S	0.77 W
manhattan	0.88 W	0.92 W	0.74 W	0.92 S	0.82 A	0.87 W
euclidean	0.88 A	0.92 A	0.77 A	0.95 S	0.84 A	0.87 A
minkowski	0.85 A	0.90 A	0.77 A	0.95 S	0.80 A	0.85 A
homological	0.76 W	0.84 W	0.58 S	1.00 S	0.64 S	0.78 S

(B) Cancer Coimbra dataset.

<b>Metric</b>	<b>F1</b>	<b>Acc.</b>	<b>Hom.</b>	<b>Comp.</b>	<b>M.Info</b>	<b>Rand</b>
bray-curtis	0.56 S	0.56 S	0.02 A	0.14 S	0.02 A	0.50 S
cosine	0.55 C	0.55 C	0.01 S	0.12 S	0.01 S	0.50 C
manhattan	0.53 S	0.53 S	0.02 A	0.13 A	0.02 A	0.50 S
euclidean	0.54 W	0.54 W	0.02 A	0.13 A	0.02 A	0.50 W
minkowski	0.53 S	0.53 S	0.02 A	0.13 A	0.02 A	0.50 S
homological	0.61 W	0.61 W	0.03 W	1.00 S	0.02 W	0.52 W

(c) Synthetic dataset with mixing.

<b>Metric</b>	<b>F1</b>	<b>Acc.</b>	<b>Hom.</b>	<b>Comp.</b>	<b>M.Info</b>	<b>Rand</b>
bray-curtis	1.00 A	1.00 A	1.00 A	1.00 A	1.38 A	1.00 A
cosine	0.83 A	0.91 A	0.72 C	0.77 S	1.38 C	0.87 A
manhattan	1.00 S	1.00 S	1.00 S	1.00 S	0.99 S	1.00 S
euclidean	1.00 A	1.00 A	1.00 A	1.00 A	1.38 A	1.00 A
minkowski	1.00 C	1.00 C	1.00 C	1.00 C	1.38 C	1.00 C
homological	0.98 A	0.99 A	0.95 A	1.00 S	1.31 A	0.98 A

complete (C), average (A), or ward (W)) with each evaluation measure. We excluded the linearly separable synthetic dataset because all of the metrics did produce the most optimal result with the appropriate linkage.

The cophenetic distance did produce best results for the Cancer dataset across the board. For the synthetic dataset with mixing, the results for the cophenetic distance appear to be on par with the other metrics even though it produced the weakest results after the cosine distance for the Iris dataset. Our results indicate that cophenetic distance does produce competitive results on measures such as the F1-score, accuracy, homogeneity and the Rand index while it shines on measures such as completeness and mutual information score consistently on all datasets. The results indicate that cophenetic distance does tend to produce complete clusters that show high average inter-class dissimilarities.

## 6. CONCLUSIONS AND FUTURE WORK

**6.1. Conclusions.** We defined a non-archimedean metric, called the cophenetic metric, on persistent homology classes. We then used this metric to sketch rooted tree presentations for zeroth persistent homology classes instead of sketching rooted trees on points in the data set. We note that having a non-archimedean metric persistent homology classes in all degrees allows one to visualize higher homology classes as dendrograms as well.

Since the zeroth homology classes naturally correspond to connected components of the subspace from which our data set is sampled, one can now compare the results of hierarchical clustering

schemes with different metrics on data points with the results we obtain from the cophenetic distance on the zeroth homology. To test the soundness of our proposal, we did numerical experiments on the geographical coordinates of a small sample cities of Turkey to compare the dendrograms coming the cophenetic metric on the zeroth homology and the dendrograms of hierarchical clustering algorithms by varying metrics in Section 5.1.

The results of our numerical experiments we outlined in Section 5.1 indicate that there is a statistically verifiable strong correlation between the dendrograms coming from the cophenetic distance matrix  $C_0(D)$  and the dendrograms coming from other metrics. The statistical evidence we collected supports our hypothesis that hierarchical clustering and zeroth persistent homology together with the cophenetic metric yield statistically verifiable commensurate topological information about the connected components of the datasets we used in our analyses.

We also note that while hierarchical clustering algorithms exclusively rely on a metric structure on the data cloud alone, persistent homology relies on the simplicial technology to derive its results, and therefore, should be impervious to the underlying metric. On the other hand, the Mantel test results in Section 4.5 indicate that cophenetic distance and Euclidean distances are most similar. This may come from the fact that Vietoris-Rips complex we used to calculate our homological invariants uses the Euclidean metric for its filtration structure.

On the practical side, one has to also check that the cophenetic distance in combination with hierarchical clustering methods does create high quality clusters. For this purpose, we compared clusters coming from hierarchical clustering algorithms on a handful of datasets with varying number of clusters using different metrics including our own cophenetic metric on the zeroth persistent homology in Section 5.2. Results we obtain indicate that cophenetic distance shines in creating high quality complete clusters where distinct clusters have low mutual information.

We notice that even though the original dataset has 3 preset clusters, Figure 7 suggests that the optimal number of clusters for the Iris dataset is 2 for all metrics while the cophenetic distance suggests that it is 4. However, one must observe that the classes *iris versicolor* and *iris virginica* are intertwined [3, 31, 33]. Our computations appear to detect this phenomenon. The cophenetic distance result suggests splitting extra subclusters along their intersection while results from other metrics suggest merging these clusters.

A similar phenomenon appears in the Cancer Coimbra dataset. In [38], the authors use logistic regression, random forests, and support vector machines to label data points as *control* or *patient* with specificity and sensitivity in the high 80%'s. Our results, on the other hand, were in the 60%'s for both specificity and sensitivity. However, we focus on using hierarchical clustering algorithms with commonly-used metrics and our cophenetic metric to split the dataset into meaningful clusters instead of labeling data points as *control* or *patient*. The results we obtained in Section 5.2 indicate that the dataset contains homogeneous meaningful subsets other than *control* and *patient*.

**6.2. Future work.** One can extend the results of this article in different directions. The first obvious avenue for extension is replacing the zeroth homology with higher persistent homology. As we noted above, dendrograms as cobordisms of 0-spheres are adequate in representing the relationships between zeroth persistent homology classes. For the higher homology classes we would need to deal with higher cobordisms of  $n$ -spheres [47] if we are to develop a similar theory for the  $n$ -th persistent homology. For the first persistent homology, the cobordisms are given by genus- $g$  Riemann surfaces with punctures. Fortunately, there is a complete classification of such surfaces in full [14]. Unfortunately, for higher dimensional homology, the cobordisms require

higher dimensional manifolds with finitely many punctures for which there is no classification exists.

The second avenue of extension we would consider is extending our result to data sets that cannot be easily embedded in an affine space. This is often the case when one deals with categorical data that require different techniques than numerical data [2]. We have shown that provided one can define a simplicial complex out of data sets whose features are purely or partially categorical, the cophenetic homological distance would yield usable information about the data set on par with hierarchical clustering.

**Acknowledgements.** The first author was supported by Research Fund Project Number TDK-2020-42698 of the Istanbul Technical University.

#### REFERENCES

- [1] Henry Adams, Tegan Emerson, Michael Kirby, Rachel Neville, Chris Peterson, Patrick Shipman, Sofya Chepushtanova, Eric Hanson, Francis Motta, and Lori Ziegelmeier, *Persistence images: A stable vector representation of persistent homology*, Journal of Machine Learning Research **18** (2017), no. 1, 218–252.
- [2] Alan Agresti, *An introduction to categorical data analysis*, Wiley Series in Probability and Statistics, John Wiley & Sons, Inc., Hoboken, NJ, 2019. Third edition of [ MR1394195]. MR3887567
- [3] Asa Ben-Hur, David Horn, Hava T. Siegelmann, and Vladimir Vapnik, *Support vector clustering*, J. Mach. Learn. Res. **2** (2002), no. 2, 125–137 (English).
- [4] J. Roger Bray and John T. Curtis, *An ordination of upland forest communities of southern wisconsin*, Ecological Monographs **27** (1957), 325–349.
- [5] Peter Bubenik, *Statistical topological data analysis using persistence landscapes*, Journal of Machine Learning Research **16** (2015), no. 1, 77–102.
- [6] Kevin Buchin, Maïke Buchin, Jaroslaw Byrka, Martin Nöllenburg, Yoshio Okamoto, Rodrigo I. Silveira, and Alexander Wolff, *Drawing (complete) binary tanglegrams: hardness, approximation, fixed-parameter tractability*, Algorithmica **62** (2012), no. 1-2, 309–332. MR2886045
- [7] Gunnar Carlsson, *Persistent homology and applied homotopy theory*, Handbook of homotopy theory, 2020, pp. 297–329.
- [8] Gunnar Carlsson and Facundo Mémoli, *Persistent clustering and a theorem of j. kleinberg*, arXiv preprint arXiv:0808.2241 (2008).
- [9] Gunnar Carlsson and Facundo Mémoli, *Characterization, stability and convergence of hierarchical clustering methods*, Journal of Machine Learning Research **11** (2010), 1425–1470. MR2645457
- [10] Gunnar Carlsson, Afra Zomorodian, Anne Collins, and Leonidas J. Guibas, *Persistence barcodes for shapes*, International Journal of Shape Modeling **11** (2005), no. 02, 149–187.
- [11] Yu-Min Chung and Austin Lawson, *Persistence curves: A canonical framework for summarizing persistence diagrams*, arXiv preprint arXiv:1904.07768 (2019).
- [12] David Cohen-Steiner, Herbert Edelsbrunner, and John Harer, *Stability of persistence diagrams*, Discrete & Computational Geometry **37** (2007), no. 1, 103–120. MR2279866
- [13] The Sage Developers, William Stein, David Joyner, David Kohel, John Cremona, and Burçin Eröcal, *Sagemath, version 9.0*, 2020.
- [14] Simon Donaldson, *Riemann surfaces*, Oxford Graduate Texts in Mathematics, vol. 22, Oxford University Press, Oxford, 2011. MR2856237
- [15] Herbert Edelsbrunner, David Letscher, and Afra Zomorodian, *Topological persistence and simplification*, Proceedings 41st annual symposium on foundations of computer science, 2000, pp. 454–463.
- [16] Yury Elkin and Vitaliy Kurlin, *The mergegram of a dendrogram and its stability*, arXiv preprint arXiv:2007.11278 (2020).
- [17] Henning Fernau, Michael Kaufmann, and Mathias Poths, *Comparing trees via crossing minimization*, Journal of Computer and System Sciences **76** (2010), no. 7, 593–608. MR2662822
- [18] Ronald A. Fisher, *The use of multiple measurements in taxonomic problems*, Annals of Eugenics **7** (1936), no. 2, 179–188.
- [19] Tal Galili, *dendextend: an R package for visualizing, adjusting and comparing trees of hierarchical clustering*, Bioinformatics **31** (2015), no. 22, 3718–3720.



- [20] Robert Ghrist, *Barcodes: the persistent topology of data*, American Mathematical Society, Bulletin, New Series **45** (2008), no. 1, 61–75. MR2358377
- [21] John A. Hartigan, *Statistical theory in clustering*, Journal of Classification **2** (1985), no. 1, 63–76. MR800514
- [22] Lawrence Hubert and Phipps Arabie, *Comparing partitions*, Journal of Classification **2** (1985), no. 1, 193–218.
- [23] Paul Samuel P Ignacio, *Intrinsic hierarchical clustering behavior recovers higher dimensional shape information*, arXiv preprint arXiv:2010.03894 (2020).
- [24] Anil K. Jain and Richard C. Dubes, *Algorithms for clustering data*, Prentice Hall Advanced Reference Series, Prentice Hall, Inc., Englewood Cliffs, NJ, 1988. MR999135
- [25] Nicholas Jardine and Robin Sibson, *Mathematical taxonomy*, John Wiley & Sons Ltd., London-New York-Sydney, 1971. Wiley Series in Probability and Mathematical Statistics. MR0441395
- [26] Stephen C. Johnson, *Hierarchical clustering schemes*, Psychometrika **32** (1967), no. 3, 241–254.
- [27] Jon M. Kleinberg, *An impossibility theorem for clustering*, Advances in neural information processing systems **32**, 2002, pp. 446–453.
- [28] Harold W Kuhn, *The hungarian method for the assignment problem*, Naval Research Logistics (NRL) **52** (2005), no. 1, 7–21.
- [29] Godfrey N. Lance and William T. Williams, *A general theory of classificatory sorting strategies: 1. hierarchical systems*, The Computer Journal **9** (1967), no. 4, 373–380.
- [30] Pierre Legendre and Louis Legendre, *Numerical ecology*, 3rd ed., Elsevier, 2012.
- [31] Alberto Lumbreras, Julien Velcin, Marie Guégan, and Bertrand Jouve, *Non-parametric clustering over user features and latent behavioral functions with dual-view mixture models*, Computational Statistics **32** (2017), no. 1, 145–177 (English).
- [32] Nathan Mantel, *The detection of disease clustering and a generalized regression approach*, Cancer research **27** (1967), no. 2 Part 1, 209–220.
- [33] Volodymyr Melnykov and Xuwen Zhu, *An extension of the K-means algorithm to clustering skewed data*, Computational Statistics **34** (2019), no. 1, 373–394 (English).
- [34] Emanuela Merelli, Matteo Rucco, Peter Sloot, and Luca Tesei, *Topological characterization of complex systems: Using persistent entropy*, Entropy **17** (2015), no. 10, 6872–6892.
- [35] Haynes Miller, *Handbook of homotopy theory*, CRC Press/Chapman and Hall Handbooks in Mathematics Series, CRC Press, Boca Raton, FL, 2020. MR4197980
- [36] Chul Moon, Noah Giansiracusa, and Nicole A. Lazar, *Persistence terrace for topological inference of point cloud data*, Journal of Computational and Graphical Statistics **27** (2018), no. 3, 576–586.
- [37] Jari Oksanen, F. Guillaume Blanchet, Michael Friendly, Roeland Kindt, Pierre Legendre, Dan McGlinn, Peter R. Minchin, R.B. O’Hara, Gavin L. Simpson, Peter Solymos, M. Henry H. Stevens, Eduard Szoecs, and Helene Wagner, *vegan: Community ecology package*, R package version 2.5-6 (2019).
- [38] Miguel Patrício, José Pereira, Joana Crisóstomo, Paulo Matafome, Manuel Gomes, Raquel Seça, and Francisco Caramelo, *Using resistin, glucose, age and bmi to predict the presence of breast cancer*, Vol. 18, BioMed Central, 2018.
- [39] Fabian Pedregosa, Gaël Varoquaux, Alexandre Gramfort, Vincent Michel, Bertrand Thirion, Olivier Grisel, Mathieu Blondel, Peter Prettenhofer, Ron Weiss, Vincent Dubourg, Jake Vanderplas, Alexandre Passos, David Cournapeau, Matthieu Brucher, Matthieu Perrot, and Édouard Duchesnay, *Scikit-learn: Machine learning in Python*, Journal of Machine Learning Research **12** (2011), 2825–2830.
- [40] R Core Team, *R: A language and environment for statistical computing*, R Foundation for Statistical Computing, Vienna, Austria, 2021.
- [41] Andrew Rosenberg and Julia Hirschberg, *V-measure: A conditional entropy-based external cluster evaluation measure*, Proceedings of the 2007 joint conference on empirical methods in natural language processing and computational natural language learning (emnlp-conll), 2007, pp. 410–420.
- [42] Peter J. Rousseeuw, *Silhouettes: A graphical aid to the interpretation and validation of cluster analysis*, Journal of Computational and Applied Mathematics **20** (1987), 53–65.
- [43] Celine Scornavacca, Franziska Zickmann, and Daniel H Huson, *Tanglegrams for rooted phylogenetic trees and networks*, Bioinformatics **27** (2011), no. 13, i248–i256.
- [44] Theodoridis Sergios and Koutroumbas Konstantinos, *Pattern recognition*, Fourth Edition, Academic Press, Boston, 2009.
- [45] Peter H.A. Sneath, Robert R. Sokal, et al., *Numerical taxonomy. the principles and practice of numerical classification.*, W.H. Freeman and Company San Francisco, 1973.
- [46] Robert R. Sokal and F. James Rohlf, *The comparison of dendrograms by objective methods*, Taxon **11** (1962), no. 2, 33–40.

- [47] Robert E. Stong, *Notes on cobordism theory*, Mathematical notes, Princeton University Press, Princeton, N.J.; University of Tokyo Press, Tokyo, 1968. MR0248858
- [48] Alexander Strehl and Joydeep Ghosh, *Cluster ensembles-a knowledge reuse framework for combining multiple partitions*, Journal of Machine Learning Research **3** (2002), no. Dec, 583–617.
- [49] Guido Van Rossum and Fred L. Drake, *Python 3 reference manual*, CreateSpace, Scotts Valley, CA, 2009.
- [50] P. Wessel, J. F. Luis, L. Uieda, R. Scharroo, F. Wobbe, W. H. F. Smith, and D. Tian, *The generic mapping tools version 6*, Geochemistry, Geophysics, Geosystems **20** (2019), no. 11, 5556–5564.
- [51] Afra Zomorodian and Gunnar Carlsson, *Computing persistent homology*, Discrete & Computational Geometry **33** (2005), no. 2, 249–274.

*Email address:* iguzel@itu.edu.tr

*Email address:* kaygun@itu.edu.tr

DEPARTMENT OF MATHEMATICS, ISTANBUL TECHNICAL UNIVERSITY, ISTANBUL, TURKEY.